

RSC Advances



This is an *Accepted Manuscript*, which has been through the Royal Society of Chemistry peer review process and has been accepted for publication.

Accepted Manuscripts are published online shortly after acceptance, before technical editing, formatting and proof reading. Using this free service, authors can make their results available to the community, in citable form, before we publish the edited article. This *Accepted Manuscript* will be replaced by the edited, formatted and paginated article as soon as this is available.

You can find more information about *Accepted Manuscripts* in the [Information for Authors](#).

Please note that technical editing may introduce minor changes to the text and/or graphics, which may alter content. The journal's standard [Terms & Conditions](#) and the [Ethical guidelines](#) still apply. In no event shall the Royal Society of Chemistry be held responsible for any errors or omissions in this *Accepted Manuscript* or any consequences arising from the use of any information it contains.

ARTICLE

Ammonia Borane - Metal Alanate composites: hydrogen desorption properties and decomposition processes

Cite this: DOI: 10.1039/x0xx00000x

Received 00th January 2012,
Accepted 00th January 2012

DOI: 10.1039/x0xx00000x

www.rsc.org/

Yuki Nakagawa,^{*a} Yudai Ikarashi,^a Shigehito Isobe,^{*ab} Satoshi Hino^a and Somei Ohnuki^a

Hydrogen desorption properties and decomposition processes of $\text{NH}_3\text{BH}_3\text{-MAIH}_4$ ($\text{M} = \text{Na, Li}$) composites were investigated by using thermogravimetry-differential thermal analysis-mass spectrometry (TG-DTA-MS), powder X-ray diffraction (XRD) and Fourier transform infrared spectroscopy (FTIR) analyses. We prepared the composites by ball-milling and the mixtures by hand-milling. The ball-milled composites desorbed 4-5 wt% hydrogen at three exothermic steps below 260 °C. The emissions of by-product gases, NH_3 , B_2H_6 and $\text{B}_3\text{H}_6\text{N}_3$, were effectively suppressed. From XRD analysis, the formation of mixed-metal (Na(Li), Al) amidoborane phase was suggested. Very different results were obtained using hand-milling. They showed only one exothermic reaction at 80-90 °C. The emission of by-product gases was not suppressed. By comparing the differences between ball-milled composites and hand-milled mixtures, the importance of mixed-metal amidoborane in this system was proposed.

1. Introduction

Hydrogen storage is a big challenge for a future hydrogen energy society. The U.S. Department of Energy (DOE) introduced a set of technical targets for on-board hydrogen storage systems in 2003.¹ Then, these were revised to the new targets in 2009.² Ultimate targets for system gravimetric and volumetric capacities of hydrogen were set to 7.5 wt% and 70 g L⁻¹, respectively.² These values are based on the tank-system, which takes into account the weight and volume of all of fuel cell components. Therefore, capacities on a materials-basis should be much larger than those on a system-basis.³ Hereafter, hydrogen capacities on a materials-basis are described. Many kinds of candidate hydrogen storage materials have been investigated, such as interstitial metal hydrides, complex hydrides, chemical hydrides and adsorbents.⁴ For example, sodium alanate (NaAlH_4) is one of complex hydrides and has a reversible hydrogen capacity of 5.6 wt%.⁴

Ammonia borane (NH_3BH_3 , AB) is one of chemical hydrides and attracts much attention as hydrogen storage materials. AB has high hydrogen capacities (19.6 wt%, 145 g L⁻¹, respectively) and desorbs hydrogen in a relatively low temperature range.⁵ Nevertheless, sluggish kinetics below 100 °C, poor recyclability, and emission of by-product gases during heating (e.g., ammonia (NH_3), diborane (B_2H_6) and borazine ($\text{B}_3\text{H}_6\text{N}_3$)) are disadvantages for practical applications.⁶⁻⁸ For instance, release of ammonia causes damage to the fuel cell performance even at trace levels.⁹ Also, NH_3 and B_2H_6 are toxic materials for living things.^{10, 11}

To overcome these disadvantages, several approaches have been developed, such as infusion of AB in nanoscaffolds,¹² doping with transition metals as catalysts,¹³ size and catalytic effects from graphitic carbon nitride,¹⁴ and chemical modification of AB by

replacing one of H atoms with an alkali or alkaline earth metal to form metal amidoboranes.¹⁵ In previous reports, many kinds of AB-MH (Metal Hydride) composites, such as AB-LiH,¹⁵⁻²⁰ AB-NaH,^{15-17,21,22} AB-KH,^{16,17,23} AB-MgH₂,²⁴⁻²⁶ AB-CaH₂,²⁴ AB-LiNH₂,²⁷ AB-LiBH₄,²⁸ and AB-Li₃AlH₆,²⁹ were synthesized and their dehydrogenation properties were investigated. Recently, AB-amine metal borohydride composites, which showed superior dehydrogenation properties, were also reported.^{30,31} In our previous report, we experimentally verified that AB-MAIH₄ ($\text{M} = \text{Na, Li}$) composites, which were prepared based on the indicator we proposed, can suppress the emission of NH_3 , B_2H_6 and $\text{B}_3\text{H}_6\text{N}_3$.³² However, their decomposition processes have not been clarified yet.

In this study, we investigated the decomposition processes of AB-MAIH₄ ($\text{M} = \text{Na, Li}$) composites. We prepared the composites by ball-milling and the mixtures by hand-milling. We analysed the hydrogen desorption properties by thermogravimetry-differential thermal analysis-mass spectrometry (TG-DTA-MS) and performed phase identification by powder X-ray diffraction (XRD) and Fourier transform infrared (FTIR) spectroscopy. By comparing the ball-milled composites and hand-milled mixtures, the decomposition processes were proposed.

2. Experimental

The starting materials NH_3BH_3 , NaAlH_4 , LiAlH_4 (purity 97 %, 90 %, 95 %, respectively) were purchased from Sigma Aldrich Co. Ltd. These materials were used as-received without any purification. All samples were handled in an argon-filled glovebox to prevent sample oxidation. AB-MAIH₄ ($\text{M} = \text{Na, Li}$) composites were prepared by ball-milling of AB and MAIH₄ ($\text{M} = \text{Na, Li}$) with a molar ratio of 1 : 1 under a 1.0

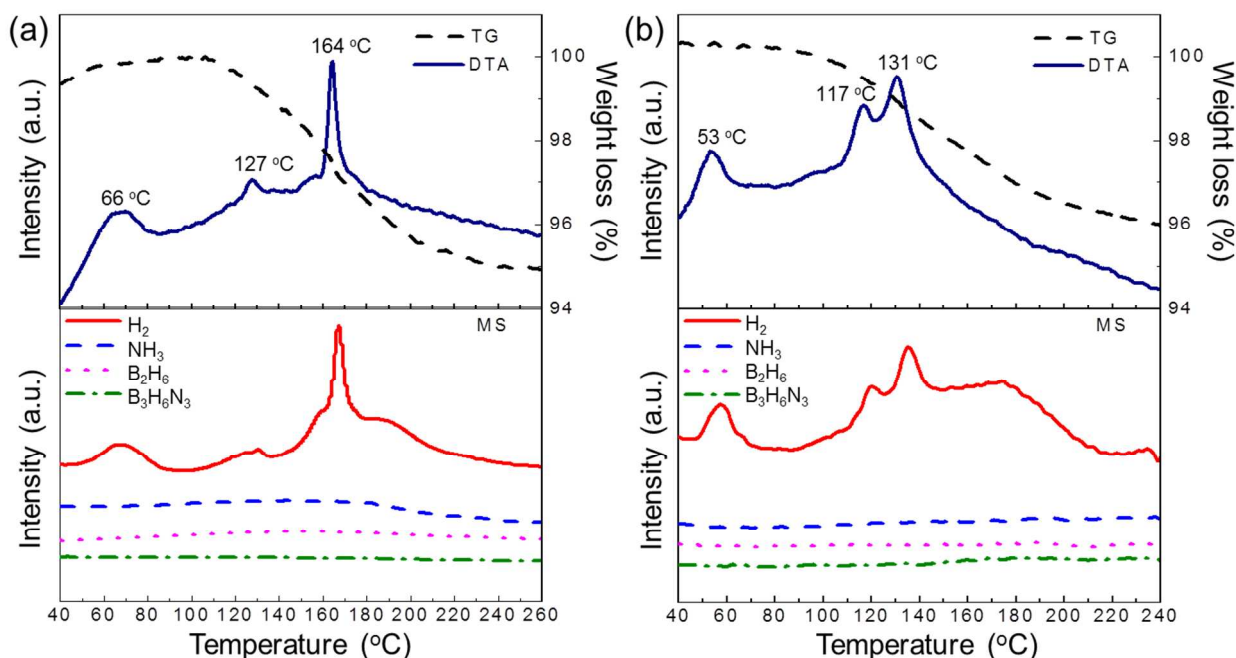


Fig. 1 TG-DTA-MS profiles of ball-milled AB-MAIH₄ composites; (a) AB-NaAlH₄ composite, (b) AB-LiAlH₄ composite. The heating rate was 5 °C min⁻¹.

MPa H₂ atmosphere with 300 rpm for 5 min. Ball-milling was performed by using a planetary ball-mill apparatus (Fritsch Pulverisette 7) with 20 stainless steel balls (7 mm in diameter) and 300 mg samples (ball : powder ratio = 70 : 1, by mass). We also prepared the mixtures by hand-milling. Hand-milled mixtures were prepared by mixing AB and MAIH₄ (M = Na, Li) in an agate mortar in the glove box for 90 seconds. Hand-milling over 120 seconds is dangerous because it often causes gas eruptions. The hydrogen desorption properties were examined by thermal desorption mass spectrometry measurements (TDMS, ULVAC, BGM-102) combined with thermogravimetry and differential thermal analysis (TG-DTA, Bruker, 2000SA). The heating rate was 5 °C min⁻¹ and the helium gas flow rate was 300 mL min⁻¹. Powder X-ray diffraction (XRD, PANalytical, X'Pert Pro with Cu K α radiation) measurements were performed to observe the phases of composites. The samples used for XRD measurements were placed on a greased glass plate in an argon-filled glovebox and then sealed with a polyimide sheet (Kapton, The Nilaco Co. Ltd.) to avoid oxidation during measurement. Fourier transform infrared spectrometry (FT-IR, Spectrum One, Perkin-Elmer) measurements were performed using a diffuse reflection cell to investigate chemical bonds in the composites. All the samples were diluted with KBr to a mass ratio of 5 : 95 (sample : KBr).

3. Results and Discussion

3.1 Hydrogen desorption properties of ball-milled composites

TG-DTA-MS results of ball-milled AB-MAIH₄ (M = Na, Li) composites are shown in Fig. 1. As shown in Fig. 1 (a), exothermic peaks were observed at 66, 127, and 164 °C in DTA profile of AB-NaAlH₄ composite. These peaks correspond to H₂ desorption peaks in mass spectra. The composite did not

desorb NH₃, B₂H₆, and B₃H₆N₃ at all within the accuracy of our apparatus. From TG profile, the amount of desorbed H₂ was estimated at 5 wt%. AB-LiAlH₄ composite showed similar H₂ desorption properties as those of AB-NaAlH₄ composite. Three exothermic peaks (53, 117 and 131 °C) were observed in DTA profile. The composite did not desorb NH₃, B₂H₆ and B₃H₆N₃. The suppression of by-product gas emission was also found in AB-Li₃AlH₆ composite.²⁹ The amount of desorbed H₂ was about 4 wt% for AB-LiAlH₄ composite. These results were quite different from the TG-DTA-MS results of AB⁶ or MAIH₄³³ (M = Na, Li) itself, suggesting the reactions between AB and MAIH₄ during milling and heating. Theoretical hydrogen capacities of AB-NaAlH₄ and AB-LiAlH₄ composites are 11.9 wt% and 14.6 wt%, respectively. H₂ desorption during ball-milling and M(BH₄) formation during heating resulted in a reduction in the amount of desorbed H₂ by TG experiments (see Section 3.2). Each exothermic peak of AB-LiAlH₄ composite was lower than the corresponding peak of AB-NaAlH₄ composite. This would be correlated with the lower thermal stability of LiAlH₄ than that of NaAlH₄.³⁴

3.2 Structure and phase analyses of ball-milled composites

The pressure increase due to H₂ desorption was observed during ball-milling, which suggested the mixed-metal amidoborane formed by the reaction between NaAlH₄ and AB. NH₃, B₂H₆, and B₃H₆N₃ desorption was not observed during ball-milling. One of the driving forces for the reaction would be the affinity of H⁻ in NaAlH₄ and H ^{δ -} in NH₃ of AB. Fig. 2 shows the XRD profiles of ball-milled AB-MAIH₄ (M = Na, Li) composites after heating to each temperature. Broad diffraction peaks at around 20° and 27° in all profiles originate from the polyimide film and grease to prevent sample oxidation. In AB-NaAlH₄ composite, both AB and NaAlH₄ phases were observed at room temperature (RT). Besides, small unknown peaks appeared in the range of 15 – 30°. These peaks don't

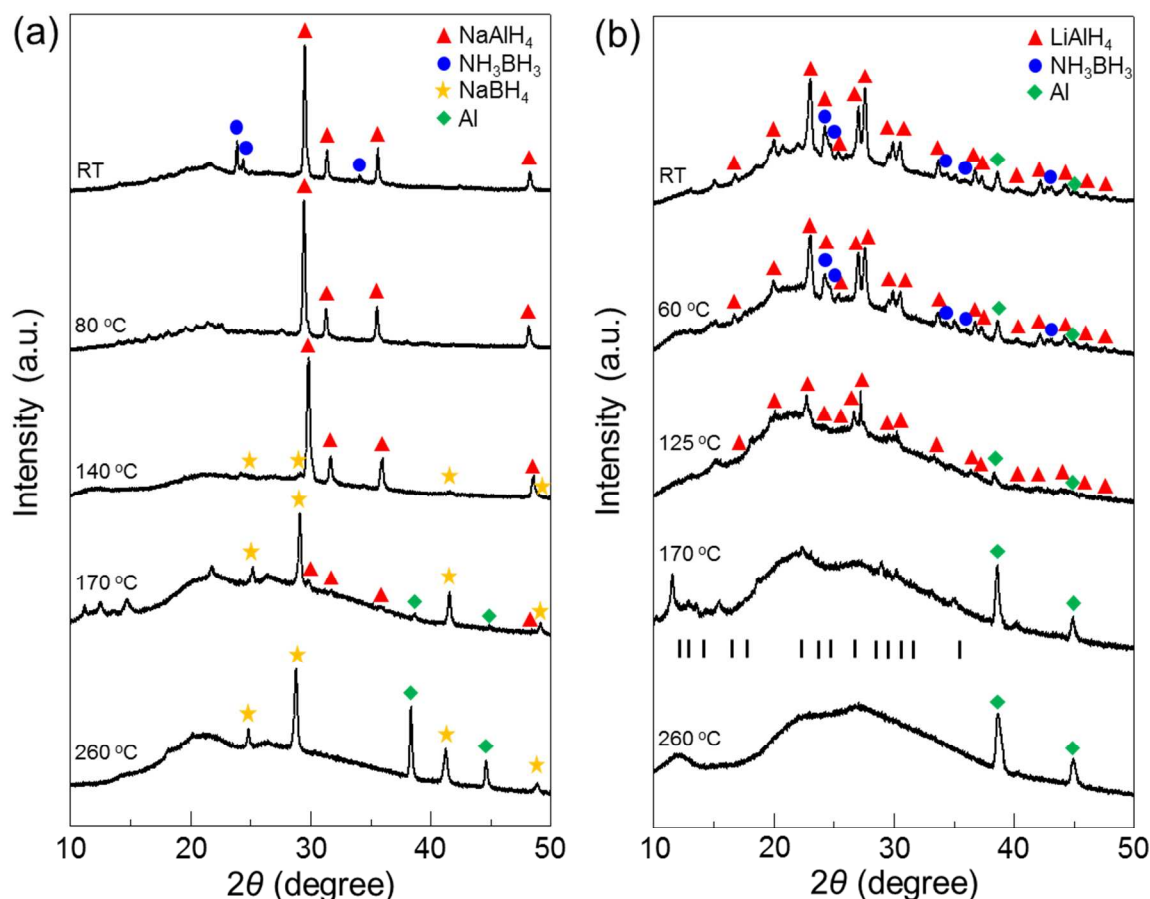


Fig. 2 XRD profiles of ball-milled AB-MAIH₄ composites after heating to each temperature; (a) AB-NaAlH₄ composite, (b) AB-LiAlH₄ composite.

match with any diffraction pattern of decomposition products of starting materials or mono-metal amidoborane, suggesting the formation of mixed-metal (Na, Al) amidoborane phase during ball-milling. After heating to 80 °C, the peak intensities of mixed-metal amidoborane became stronger compared to RT. The reaction between AB and NaAlH₄ proceeded further to form the mixed-metal amidoborane, resulting in the H₂ desorption at 66 °C as shown in Fig. 1 (a). After heating to 140 °C, the mixed-metal amidoborane phase disappeared, indicating its decomposition. It is interesting that NaBH₄ phase appeared at 140 °C. After heating to 170 °C, strong peak intensities of NaBH₄ were observed, while most of NaAlH₄ phase disappeared. The formation process of NaBH₄ will be described in Section 3.3. Furthermore, a new set of peaks were observed in the range of 10 – 25°. This could be another mixed-metal amidoborane formed by the reaction between Na₃AlH₆ and AB. After heating to 260 °C, this unknown phase decomposed and only NaBH₄ and Al phases were observed. In case of AB-LiAlH₄ composite, similar results were obtained as AB-NaAlH₄ composite. At RT, unknown peaks, which were considered as mixed-metal (Li, Al) amidoborane, were observed in the range of 10 – 25°. After heating to 170 °C, further new peaks were observed in the range of 10 – 40°. The peak positions of AB-Li₃AlH₆ composite reported by Xia *et al.* were also shown as reference in Fig. 2 (b).²⁹ The positions of observed peaks were similar to the reference, suggesting the formation of mixed-metal (Li, Al) amidoborane. Though borohydride phase was not observed in the XRD profiles of AB-LiAlH₄ composite, the

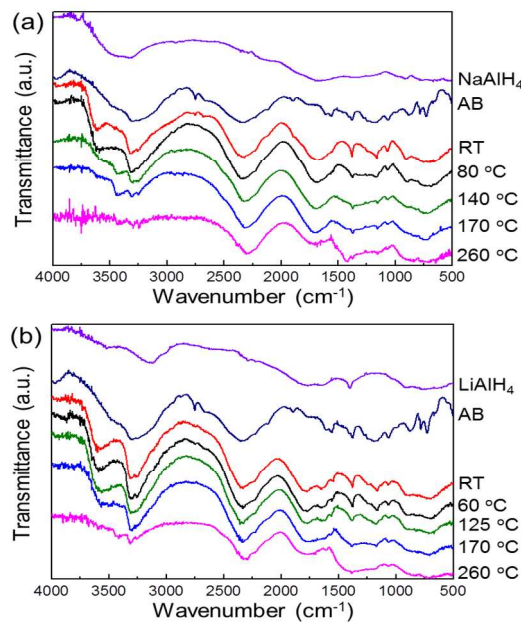


Fig. 3 *In-situ* FTIR spectra of ball-milled AB-MAIH₄ composites at each temperature; (a) AB-NaAlH₄ composite, (b) AB-LiAlH₄ composite. AB and MAIH₄ (M = Na, Li) spectra was presented for comparison. The heating rate was 5 °C min⁻¹.

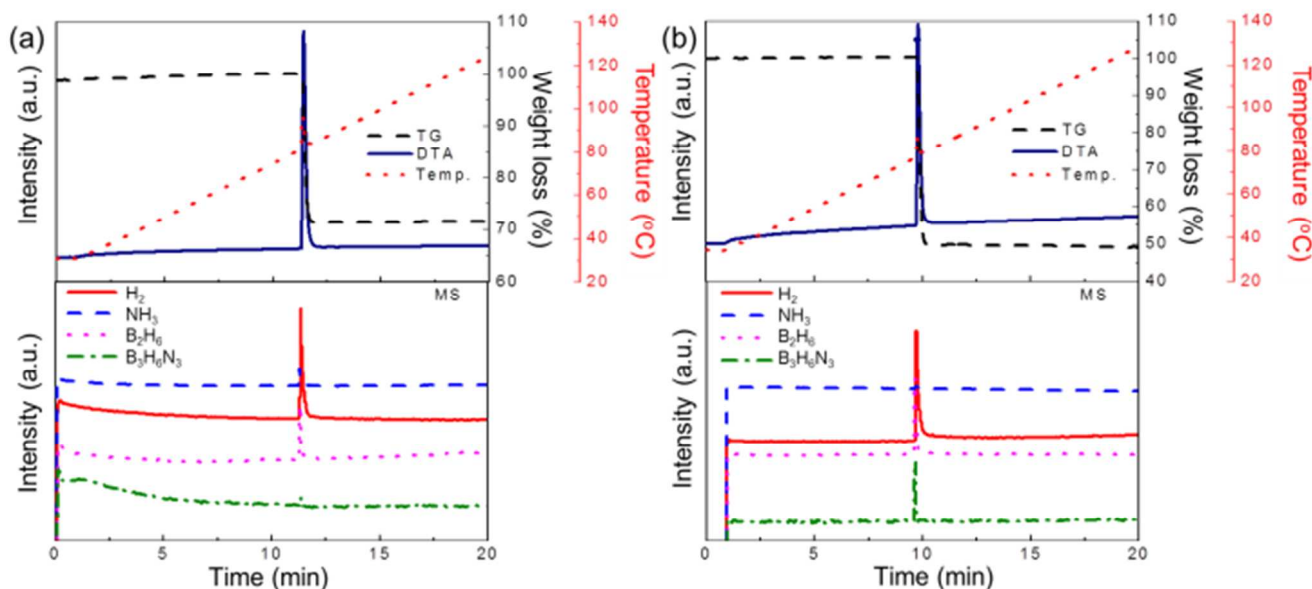


Fig. 4 TG-DTA-MS profiles of hand-milled AB-MAIH₄ mixtures; (a) AB-NaAlH₄ mixture, (b) AB-LiAlH₄ mixture. The heating rate was 5 °C min⁻¹.

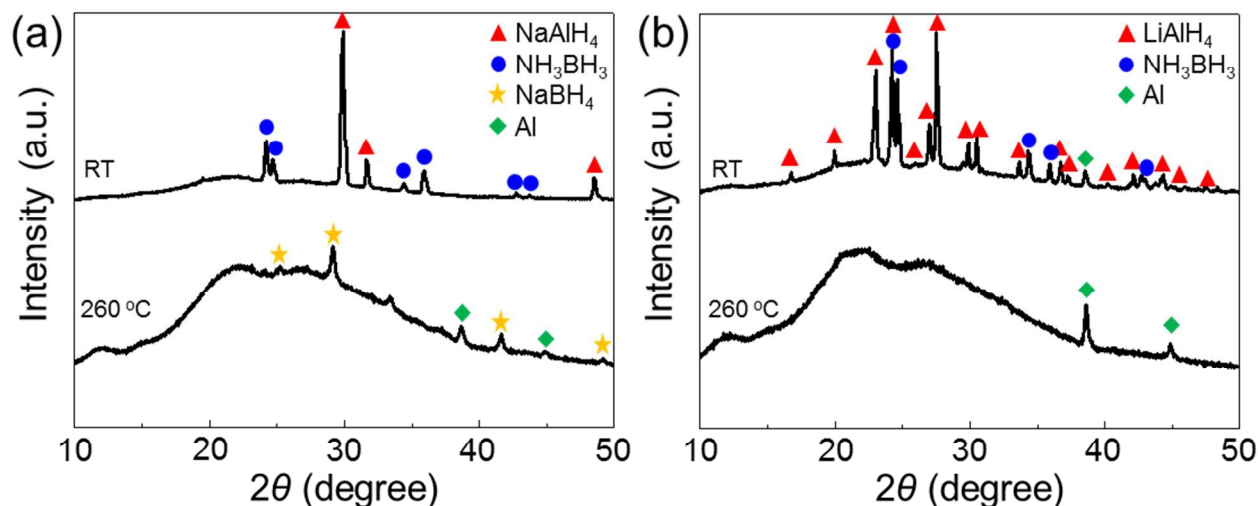


Fig. 5 XRD profiles of hand-milled AB-MAIH₄ mixtures at RT and after heating to 260 °C; (a) AB-NaAlH₄ mixture, (b) AB-LiAlH₄ mixture.

FTIR spectra (Fig. 3 (b)) showed the strong B-H stretching. This indicated that the amorphous LiBH₄ formed during heating.

Fig. 3 shows the *in-situ* FTIR spectra of ball-milled AB-MAIH₄ (M = Na, Li) composites during heating. The spectra of AB and MAIH₄ (M = Na, Li) at RT were also shown as references. In AB-MAIH₄ (M = Na, Li) composites, peak intensities corresponding to N-H stretching between 3150 and 3500 cm⁻¹ decreased as temperature increased, whereas peaks corresponding to B-H stretching between 2200 and 2400 cm⁻¹ were remained after heating to 260 °C in both composites. This phenomenon was also observed in other metal amidoboranes.^{21,24,25,28,29} A new compound containing nitrogen would be formed during H₂ desorption.

3.3 Comparison with hand-milled mixtures

To clarify the reaction process in detail, we prepared the mixtures by hand-milling and investigated their H₂ desorption properties and phases. Interestingly, results were quite different from the ball-milled composites. Fig. 4 shows TG-DTA-MS results of hand-milled AB-MAIH₄ (M = Na, Li) mixtures. Sharp exothermic peaks were observed at 90 °C (AB-NaAlH₄) and 84 °C (AB-LiAlH₄) in DTA profiles. The weight losses of about 30 wt% (AB-NaAlH₄) and 50 wt% (AB-LiAlH₄) were also observed. From the mass spectra, H₂, NH₃, B₂H₆ and B₃H₆N₃ peaks were observed in both mixtures. Except this exothermic reaction, any reactions were not observed up to 260 °C.

Fig. 5 shows the XRD profiles of hand-milled AB-MAIH₄ (M = Na, Li) mixtures before and after heating to 260 °C. Before heating, AB and MAIH₄ (M = Na, Li) were observed. Unknown peaks were not observed in the range of 10 – 30°, which was different from the results of ball-milled composites.

After heat treatment, NaBH₄ was observed in the AB-NaAlH₄ mixture, which was similar to the results of ball-milled composites.

The reaction observed in the hand-milled mixture was quite similar to the solid state reaction of MAIH₄ (M = Na, Li) with NH₄Cl. In this reaction, MCl and [H₄Al·NH₄] is formed and soon [H₄Al·NH₄] decomposes to [HAlNH] and H₂, accompanied by a large exothermic heat.³⁵ The previous study showed diammoniate of diborane (DADB), [(NH₃)₂BH₂]⁺[BH₄]⁻, an ionic isomer of AB, is formed during the induction period before H₂ desorption occurs.³⁶ MAIH₄ was also confirmed to be an ionic compound, consisting of M⁺ cation and AlH₄⁻ anion.³⁷ Considering the reaction between DADB and NaAlH₄, the reaction between BH₄⁻ anion and Na⁺ cation would cause the formation of NaBH₄. On the one hand, the reaction between [(NH₃)₂BH₂]⁺ and AlH₄⁻ would cause the H₂ and by-product gas emissions. However, the ball-milled composites showed the different results from the hand-milled mixtures. This would be attributed to the formation of mixed-metal amidoborane. Though this phase was not observed in the hand-milled mixtures, it was observed in the ball-milled composites at not only RT but also other temperatures (e.g., 170 °C). The interaction between metal amidoborane and AB like LiNH₂BH₃·NH₃BH₃ showed the significantly low H₂ desorption temperature.^{19,20} Similarly, the interaction between mixed-metal amidoborane and AB could occur in the ball-milled composites. Mixed-metal amidoborane would stabilize the reaction between Al-H bonds and N-H bonds, resulting in the suppression of by-product gases. Thus, it is suggested that mixed-metal amidoborane plays an important role in suppressing the emission of by-product gases.

4. Conclusions

AB-MAIH₄ (M = Na, Li) composites were successfully synthesized by ball-milling and their hydrogen desorption properties and decomposition processes were investigated. The composites desorbed 4-5 wt% hydrogen below 260 °C, accompanied by H₂ desorption. They did not desorb NH₃, B₂H₆, and B₃H₆N₃ at all. They showed three exothermic reactions below 260 °C, accompanied by H₂ desorption. The first reaction is ascribed to the formation of mixed-metal amidoborane phase. The second reaction is ascribed to the decomposition of mixed-metal amidoborane. In the last, the reactions described as below occurred. One is the reaction between AB and MAIH₄ (M = Na, Li), which result in the formation of MBH₄ (M = Na, Li). The other is the reaction between M₃AlH₆ (M = Na, Li) and AB, which result in the formation of another mixed-metal amidoborane. The hand-milled mixtures showed quite different results from the ball-milled composites. They showed only one exothermic reaction at 80-90 °C. The emission of by-product gases was not suppressed. By comparing the results of the ball-milled composites with those of the hand-milled mixtures, the importance of the mixed-metal amidoborane as a barrier against by-product gas emission in this system was proposed. These results would be helpful for clarifying reaction mechanisms of AB-MH composites.

Notes and References

^a Graduate School of Engineering, Hokkaido University, N-13, W-8, Sapporo 060-8278, Japan. E-mail: isobe@eng.hokudai.ac.jp (S. Isobe), y-nakagawa@eng.hokudai.ac.jp (Y. Nakagawa); Tel: +81-11-706-6771; FAX: +81-11-706-6772

^b Creative Research Institution, Hokkaido University, N-21, W-10, Sapporo 001-0021, Japan

- S. Satyapal, J. Petrovic, C. Read, G. Thomas and G. Ordaz, *Catal. Today*, 2007, **120**, 246-256.
- http://www1.eere.energy.gov/hydrogenandfuelcells/storage/pdfs/target_s_onboard_hydro_storage_explanation.pdf
- J. Yang, A. Sudik, C. Wolverton and D. J. Siegel, *Chem. Soc. Rev.*, 2010, **39**, 656-675.
- U. Eberle, M. Felderhoff and F. Schüth, *Angew. Chem. Int. Ed.*, 2009, **48**, 6608-6630.
- F. H. Stephens, V. Pons and R. T. Baker, *Dalton Trans.*, 2007, **25**, 2613-2626.
- G. Wolf, J. Baumann, F. Baitalow and F. P. Hoffmann, *Thermochim. Acta*, 2000, **343**, 19-25.
- F. Baitalow, J. Baumann, G. Wolf, K. J. Rößler and G. Leitner, *Thermochim. Acta*, 2002, **391**, 159-168.
- J. Baumann, F. Baitalow and G. Wolf, *Thermochim. Acta*, 2005, **430**, 9-14.
- N. Rajalakshmi, T. T. Jayanth and K. S. Dhathathreyan, *Fuel Cells*, 2004, **3**, 177-180.
- International Chemical Safety Cards, ICSC number: 0414.
- International Chemical Safety Cards, ICSC number: 0432.
- A. Gutowska, L. Li, Y. Shin, C. M. Wang, X. S. Li, J. C. Linehan, R. S. Smith, B. D. Kay, B. Schmid, W. Shaw, M. Gutowski and T. Autrey, *Angew. Chem. Int. Ed.*, 2005, **44**, 3578-3582.
- B. L. Conley, D. Guess and T. J. Williams, *J. Am. Chem. Soc.*, 2011, **133**, 14212-14215.
- Z. Tang, X. Chen, H. Chen, L. Wu and X. Yu, *Angew. Chem. Int. Ed.*, 2013, **52**, 5832-5835.
- Z. Xiong, C. K. Yong, G. Wu, P. Chen, W. Shaw, A. Karkamkar, T. Autrey, M. O. Jones, S. R. Johnson, P. P. Edwards and W. I. F. David, *Nat. Mater.*, 2008, **7**, 138-141.
- A. T. Luedtke and T. Autrey, *Inorg. Chem.*, 2010, **49**, 3905-3910.
- Y. Zhang and C. Wolverton, *J. Phys. Chem. C*, 2012, **116**, 14662-14664.
- K. Shimoda, K. Doi, T. Nakagawa, Y. Zhang, H. Miyaoka, T. Ichikawa, M. Tansho, T. Shimizu, A.K. Burrell and Y. Kojima, *J. Phys. Chem. C*, 2012, **116**, 5957-5964.
- C. Wu, G. Wu, Z. Xiong, W. I. F. David, K. R. Ryan, M. O. Jones, P. P. Edwards, H. Chu and P. Chen, *Inorg. Chem.*, 2010, **49**, 4319-4323.
- C. Wu, G. Wu, Z. Xiong, X. Han, H. Chu, T. He and P. Chen, *Chem. Mater.*, 2010, **22**, 3-5.
- K. J. Fijałkowski and W. Grochala, *J. Mater. Chem.*, 2009, **19**, 2043-2050.
- K. Shimoda, Y. Zhang, T. Ichikawa, H. Miyaoka and Y. Kojima, *J. Mater. Chem.*, 2011, **21**, 2609-2615.
- H. V. K. Diyabalanage, T. Nakagawa, R. P. Shrestha, T. A. Semelsberger, B. L. Davis, B. L. Scott, A. K. Burrell, W. I. F. David, K. R. Ryan, M. O. Jones and P. P. Edwards, *J. Am. Chem. Soc.*, 2010, **132**, 11836-11837.
- Y. Zhang, K. Shimoda, H. Miyaoka, T. Ichikawa and Y. Kojima, *Int. J. Hydrogen Energy*, 2010, **35**, 12405-12409.
- X. Kang, L. Ma, Z. Fang, L. Gao, J. Luo, S. Wang and P. Wang, *Phys. Chem. Chem. Phys.*, 2009, **11**, 2507-2513.
- J. Luo, Z. Kang and P. Wang, *Energy Environ. Sci.*, 2013, **6**, 1018-1025.
- K. R. Graham, T. Kemmitt and M. E. Bowden, *Energy Environ. Sci.*, 2009, **2**, 706-710.
- J. Luo, H. Wu, W. Zhou, X. Kang, Z. Fang and P. Wang, *Int. J. Hydrogen Energy*, 2012, **37**, 10750-10757.
- G. Xia, Y. Tan, X. Chen, Z. Guo, H. Liu, and X. Yu, *J. Mater. Chem. A*, 2013, **1**, 1810-1820.
- Y. Tan, Q. Gu, J. A. Kimpton, Q. Li, X. Chen, L. Ouyang, M. Zhu, D. Sun and X. Yu, *J. Mater. Chem. A*, 2013, **1**, 10155-10165.
- X. Chen, F. Yuan, Q. Gu and X. Yu, *Dalton Trans.*, 2013, **42**, 14365-14368.
- Y. Nakagawa, S. Isobe, Y. Ikarashi and S. Ohnuki, *J. Mater. Chem. A*, 2014, **2**, 3926-3931.

- 33 T. Zhang, S. Isobe, Y. Wang, H. Oka, N. Hashimoto and S. Ohnuki, *J. Mater. Chem. A*, 2014, **2**, 4361-4365.
- 34 T. Matsunaga, F. Buchter, K. Miwa, S. Towata, S. Orimo and A. Züttel, *Renewable Energy*, 2008, **33**, 193-196.
- 35 H. Zhang, Y. S. Loo, H. Geerlings, J. Lin and W. S. Chin, *Int. J. Hydrogen Energy*, 2010, **35**, 176-180.
- 36 A. C. Stowe, W. J. Shaw, J. C. Linehan, B. Schmid and T. Autrey, *Phys. Chem. Chem. Phys.*, 2007, **9**, 1831-1836.
- 37 H. W. Brinks and B. C. Hauback, *J. Alloys Compd.*, 2003, **354**, 143-147.